




# Landslide Susceptibility Model by Means of Remote Sensing Images and AutoML

Diego Renza<sup>1</sup>(✉) , Elsa Adriana Cárdenas<sup>1</sup>, Carlos Marcelo Jaramillo<sup>1</sup>,  
Serena Sarah Weber<sup>2</sup>, and Estibaliz Martínez<sup>3</sup>

<sup>1</sup> Universidad Militar Nueva Granada, Bogotá, Colombia  
{diego.renza, elsa.cardenas}@unimilitar.edu.co

<sup>2</sup> Universidad Católica de Manizales, Manizales, Colombia  
sweber@ucm.edu.co

<sup>3</sup> Universidad Politécnica de Madrid, España, Spain  
emartinez@fi.upm.es

**Abstract.** Hydrometeorological phenomena, including mass movements, are a frequent threat that can generate a great impact at different levels. In order to estimate the susceptibility to mass movements, this work contains a new proposal to estimate the susceptibility to mass movements using a supervised learning algorithm designed from AutoML (Automated machine learning). Pixel-level information from Sentinel-2 multispectral images was used to train the model, and an expert's susceptibility map was used as labels.

**Keywords:** Landslide · Susceptibility · AutoML · Autokeras

## 1 Introduction

Hydrometeorological phenomena, including mass movements, are one of the most frequent hazards that cause a large number of deaths and damage to infrastructure around the world. Particularly in Colombia, 88% of disasters are associated with the occurrence of this type of events, where about 14% of the affected houses, as well as 66% of deaths are associated with mass movements [16].

Therefore, in order to mitigate the effects generated by the occurrence of these events and to carry out a more efficient management of the territory, several types of methodologies have been proposed to assess the susceptibility to landslides, whose application depends on aspects related to the type of movements, the scale of work, the information available and the level of experience of those performing these analyses.

The main methods used in the assessment of mass movements described by [6] include Landslide susceptibility maps based on a combination of geological, topographical and land-cover conditions, inventory-based and knowledge driven methods, quantitative data-driven methods and physically based models. The heuristic method involves the direct intervention of experts to determine the susceptibility in the field or from geological and geomorphological information

of the terrain, using GIS (Geographic Information System) tools for the elaboration of the final map. There are also bivariate, multivariate and artificial neural network-based statistical methods, as well as physical methods for assessing susceptibility to mass movement obtained from modeling slope failure processes.

Several of the studies carried out involve the use of techniques such as remote sensing. Techniques used include visual interpretation and digital analysis of aerial photographs and satellite images [3,7,8], supervised classification methods to differentiate hill-slope landslides from other terrain units [15], and use of high resolution and image fusion for landslide risk assessment [13,17].

Likewise, different types of analysis have been carried out to improve the detection processes of this type of phenomenon. For instance, the analysis of conventional methods for landslide mapping including geomorphological inventories of seasonal and multitemporal events and the application of other recent technologies involving high-resolution digital elevation models [9], analysis of the influence of tectonics on the progressive erosion of landscapes and propose a method for the classification of landscapes according to their erosional stage from the combination of geomorphic indices based on digital elevation models (DEMs) [1], the use of a joint probability model to show a measure of future landslide hazard using five model estimation procedures applied to the Chinchiná river basin, department of Caldas, Colombia [5], or the use of object oriented classification (OOA) with high resolution images to detect mass movements [12].

With respect to the use of artificial intelligence methods, different approaches have been proposed, such as the use of residual networks for landslide detection employing spectral and topographic information [19] or the use of ensemble methods [23]. For example, the assembled boosting models presented the best values in terms of performance and predictive capacity in an evaluation of machine learning methods in the vicinity of a hydrographic basin in Colombia [14].

Considering the above, this paper contains a new proposal for mass movement susceptibility using an artificial intelligence algorithm. The AutoML (Automated Machine Learning) algorithm is trained using as label the susceptibility map made by an expert from geological, geomorphological information and the use of GIS tools, and as attributes the pixel level information from Sentinel-2A multispectral images. This method is presented as an alternative to evaluate landslide susceptibility in areas where there is a lack of information such as slopes, geological or geomorphological data.

## 2 Study Area

The study area includes a region between “San Luis de Gaceno” and “Santa María” at the Department of Boyacá (Colombia). The geographical zone cover an area of 300 km<sup>2</sup>; the upper left corner of the zone is placed at 4°54′44.02″N, −73°21′22.15″W, whereas the lower right corner is placed at 4°46′35.62″N, −73°10′34.46″W. The locator map is shown in Fig. 1. In the study zone, most of the area corresponds to forest cover (approximately 55%), while pasture cover

corresponds to approximately 35% of the study area, and the remaining percentage is soil.

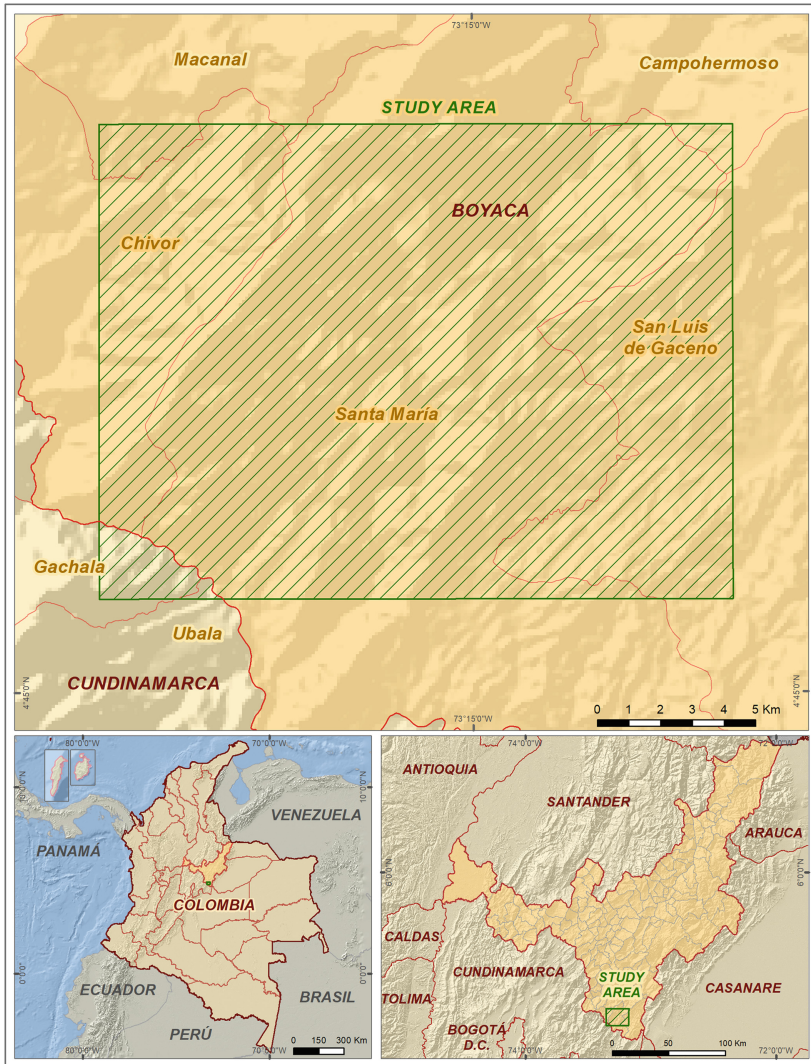


**Fig. 1.** Location of the study area corresponding to “San Luis de Gaceno” and “Santa María” at the Department of Boyacá (Colombia).

Once the study area has been defined, and in order to use remote sensing data, it is necessary to define the type of sensor to be used and the image bands to be selected as attributes within a machine learning model. Similarly, in order to train the supervised learning method, it is necessary to obtain a reference map (ground truth) that defines the labels of the data. These issues are presented below.

### 3 Image Data

Given that the determination of areas with susceptibility to landslide is a phenomenon that depends on geological, geomorphological and land cover aspects, it is necessary to consider images that include bands in different regions of the electromagnetic spectrum (ultraviolet, visible, infrared).

According to the above, a multispectral image of Sentinel-2 sensor captured in January of 2016 was selected for the study area. This image has  $998 \times 750$  pixels, and it contains 13 spectral bands, including visible, Near Infra-Red (NIR), and Short Wave Infra-Red (SWIR) bands. Of the 13 bands, four have a spatial resolution of 10 meters, six bands have a resolution of 20 meters and three have a resolution of 60 meters. The radiometric resolution of the Sentinel 2 images is 12-bits, and the intensities are stored as 16-bits integers in the final product. The true color composition of the multispectral image is shown in Fig. 2a, and the general information of Sentinel-2 bands is shown in Table 1.

**Table 1.** Sentinel-2 bands.

Band	Description	Wavelength (nm)	Resolution
B1	Coastal aerosol	~ 443	60
B2	Blue	~ 493	10
B3	Green	~ 560	10
B4	Red	~ 665	10
B5	Vegetation Red edge	~ 704	20
B6	Vegetation Red edge	~ 740	20
B7	Vegetation Red edge	~ 783	20
B8	NIR	~ 833	10
B8A	Vegetation Red edge	~ 865	20
B9	Water vapour	~ 945	60
B10	Cirrus detection	~ 1374	60
B11	SWIR 1	~ 1610	20
B12	SWIR 2	~ 2190	20

### 4 Materials and Methods

The identification scheme for landslide susceptible zones is based on a supervised classification model, so it is necessary to build the reference data that will be used for training the model (ground truth), define the features that will be used in the model from the image data, and define the structure of the machine learning model that will be trained using the labels and attributes previously defined. The construction of these labels, the definition of the features and the characteristics of the proposed model are explained below.

#### 4.1 Ground Truth Data

In order to define the reference labels that can be used to train, select and evaluate a machine learning model, a consolidated methodology was used. The susceptibility to landslide in the study area was determined by applying elements of the methodology proposed in [20,21]. The application of these methodologies allows estimating a map of susceptibility to landslide phenomena from the crossing of weighted thematic layers (variables), based on the density of unstable processes and their degree of influence.

Susceptibility to landslide is subject to several factors such as the lithological composition of the rock (geology), the denudational environment in which it is formed (geomorphology) and the type of land use that is being given to this area (land cover). The combination of these factors determines the occurrence of landslide, always taking into account the variation of the terrain, the morphogenetic environments and the degree of humidity and infiltration in the area that can affect the resistance of the material.

The variation of the lithological and structural characteristics of the study area influences the process of landslide generation, since they lead to differences in the resistance and permeability of rocks and soils. For the determination of susceptibility by geologic factor, three weighted thematic layers were assigned as shown in Eq. 1.

$$G = 0.25R + 0.25T + 0.5F_D \quad (1)$$

Where,  $G$  is the susceptibility by geologic factor,  $R$  (resistance) measures the resistance of the rocks to weathering,  $T$  (Texture) is the variable that establishes the differences in the rocks in terms of strength and directionality of mechanical properties, and  $F_D$  (fracture density) measures the regional structural discontinuities in the rock masses that decrease their resistance, increasing susceptibility to the occurrence of landslide.

Regarding geomorphology, the geomorphological units generated by the Colombian Geological Service were taken, making a more detailed delimitation of these units using a digital elevation model with a spatial resolution of 12.5 m and satellite images of the study area. Subsequently, this element was qualified according to its morphogenesis (origin of landforms, i.e., the causes and processes that shaped the landscape [20]). The susceptibility by geomorphology factor is given by Eq. 2.

$$G_m = 0.4M_g + 0.6M_m \quad (2)$$

Where  $G_m$  is the susceptibility by geomorphology factor,  $M_g$  is the morphogenesis, and  $M_m$  is the morphometry.

Regarding land use, the type of vegetation cover and land use influence soil stability, as they can reflect soil infiltration capacity and soil moisture, as well as increased resistance due to the presence of roots and protection against erosion. With respect to urban areas, there is generally no good wastewater management, hence surface runoff can increase erosion and consequently instability. In general, it can be said that the areas where most movements occur are directly related to soils without cover or bare soils, as well as the areas with the steepest slopes.

Finally, the total susceptibility was calculated from the weighting of the susceptibility obtained for geology ( $G$ ), geomorphology ( $G_m$ ) and cover ( $C$ ) factors (Eq. 3).

$$S = 0.2G + 0.6G_m + 0.2C \quad (3)$$

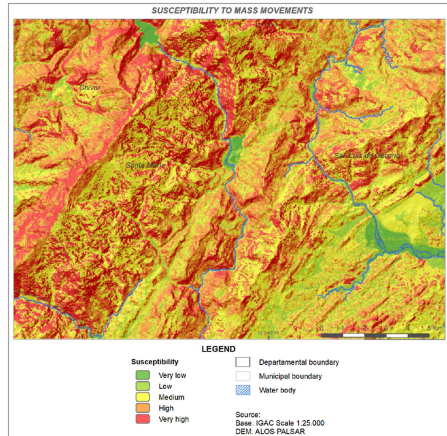
In addition, taking into account that geology, geomorphology and cover factors were rated from 1 to 5, the susceptibility of the final map is also defined on the same scale, where 5 relates to the highest susceptibility. The landslide susceptibility map of the study area is shown in Fig. 2b. In this map there is a high percentage of areas with high susceptibility, mainly from the central zone to the north-west, while from the central zone to the south-east, the susceptibility presents mostly areas of medium and low susceptibility.

The map shown in Fig. 2b was obtained from the analysis of susceptibility and threat due to landslide for the study area and was carried out by an expert supported by GIS tools. The spatial and dynamic relationship of the information was made from the collection of information and observations of variables. The complexity of obtaining this type of maps leads to the evaluation of automatic learning tools that make use of easily accessible data. The following section shows the proposal for data selection to perform this task.

In accordance with the above, the susceptibility value obtained is taken as ground truth and will be used in the training process as the label for the selected attributes, as well as the label for evaluating the proposed model.



(a) Multispectral Sentinel-2 Image. 300 km<sup>2</sup> (998 × 750 pixels), RGB color composition. “San Luis de Gaceno” and “Santa María” at the Department of Boyacá (Colombia). The upper left corner is placed at 4°54′44.02″N, -73°21′22.15″W.



(b) Landslide movement susceptibility map (Ground truth)

**Fig. 2.** Image data and Ground truth data.

## 4.2 Structured Data (Input for the AutoML Model)

Although satellite images can be considered unstructured data (i.e., they do not have a rigid structure like tabular data), in this research the image was converted to structured data by considering pixel-level information. Accordingly, for each pixel position, the input attributes correspond to the pixel values of each of the image bands (i.e. the bands shown in Table 1). Having the data structured in this way (i.e., from a multispectral image) ensures that there are no null data, categorical data, or outlier data. It should be noted that bands 1, 9 and 10 were not considered as input attributes due to their low spatial resolution (60 m).

Therefore, the attributes initially selected correspond to bands 2, 3, 4 and 8 (10 m), and bands 5, 7, 8A, 11 and 12 (20 m) of Sentinel-2 Image. From these georeferenced bands of different pixel size, a new multiband file was formed, in which the 10 m bands were resampled to 20 m (nearest neighbor) maintaining the UTM WGS-84 projection.

In addition, the five susceptibility levels shown in the map in Fig. 2b were reduced to two classes: high susceptibility (for values of 5), and moderate susceptibility (for values between 1 and 4). Thus, the attributes to be evaluated include 9 bands of the original image, and the problem can be approached as a binary classification problem.

Since the input image ( $998 \times 750$  pixels) is being processed at the pixel level, the total number of examples available to train, validate and test the model is 748500 examples. Samples from this dataset were randomized and split, involving 80% samples (598800) for training, 10% samples (74850) for validation (used to tune hyperparameters) and 10% samples (74850) for testing.

## 4.3 AutoML Model

Automated Machine Learning (AutoML) consists of solutions to automate tasks that apply machine learning to any type of problem. AutoML solutions can include different phases of the process, from data processing to model retrieval. AutoKeras is an AutoML system based on Keras, looking for make machine learning accessible to everyone; it was developed by DATA Lab at Texas A&M University [11]. AutoKeras supports several tasks, such as image classification, image regression, text classification, text regression, structured data classification and structured data regression. This tool also allows to build customized models, specifying the high-level architecture, so that AutoKeras performs a search for the best configuration (hyperparameters).

For the present investigation, the AutoKeras AutoModel option was used, which allows defining the model according to the inputs and outputs, i.e. AutoModel infers the rest of the model. The model is fitted from a hyperparameter search space, and the fitted model can then be used as any Keras model (e.g., prediction or evaluation) [4].

To configure the AutoModel, the input was defined as structured data, and the output as a classification type. The number of trials was set to 100, the batch size to 32, the number of epochs to train each model to 10, and the

search space (automatically defined by AutoKeras) involved the hyperparameters shown in Table 2. In AutoKeras, a greedy search algorithm is used to select the hyperparameters in the space, which evaluates a list of models recursively, always selecting the best model and building a hyperparameter tree from it. Once evaluated, it can generate a new set of hyperparameter values by replacing the previous ones. The evaluation and selection of the best model is repeated until the maximum number of trials is reached. This search process is greedy as it always selects the current best model and generates new models in its neighborhood [10].

**Table 2.** Hyperparameters in the search space for the AutoModel.

Hyperparameter	Values in search space	Best value
Normalization	[False, True]	True
Batch normalization	[False, True]	True
No. of layers	[1, 2, 3]	3
No. of units (Layer 1)	[16, 32, 64, 128, 256, 512, 1024]	256
Dropout (Layer 1)	[0.0, 0.25, 0.5]	0.0
No. of units (Layer 2)	[16, 32, 64, 128, 256, 512, 1024]	256
Dropout (Layer 2)	[0.0, 0.25, 0.5]	0.0
No. of units (Layer 3)	[16, 32, 64, 128, 256, 512, 1024]	32
Dropout (Layer 3)	[0.0, 0.25, 0.5]	0.25
Optimizer	[Adam, SGD, Adam weight decay]	Adam weight decay
Learning rate	[0.1, 0.01, 0.001, 0.0001, 2e−05, 1e−05]	0.001

After searching for the best model and the best hyperparameters for the AutoModel, based on the performances in the validation data, the model shown in Fig. 3 was obtained. The best model was obtained from the hyperparameter configuration shown in Table 2 (column 3). The description of the model and its layers is shown in Table 3. Accordingly, the model includes an input data normalization layer, batch normalization to accelerate network convergence, 2 fully connected layers of 256 units without dropout, followed by a fully connected layer of 32 units with dropout of 0.25 to reduce overfitting, an Adam optimizer with weight decay and a learning rate of 0.001 was used to train the best model.



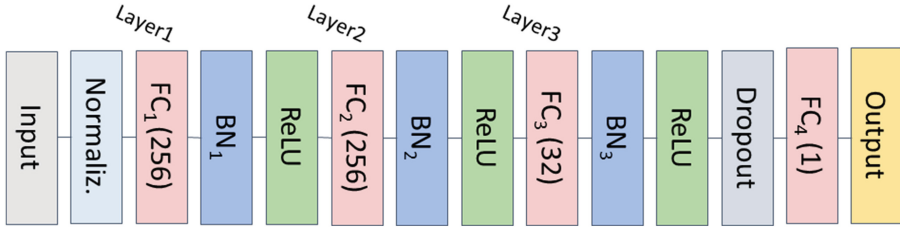


**Fig. 3.** Architecture of the model obtained with AutoKeras. FC: Fully Connected (Dense) layer, BN: Batch Normalization, ReLU: Rectified Linear Unit activation function.

The number of trainable parameters of the model can be seen in Table 3. In each fully connected layer, this value is calculated by taking the number of units of the previous layer (or number of inputs) multiplied by the number of units of the layer, plus the number of units of the layer. The total number of trainable parameters thus equals 77,953 (including batch normalization parameters) and the number of non-trainable parameters is 1,109.

**Table 3.** Summary of the model obtained with AutoKeras

Layer	No. of units	Output shape	Trainable parameters
Input	-	(,10)	0
Normalization	-	(,10)	21
$FC_1$ (Dense)	256	(,256)	2816
$BN_1$ (Batch normalization)	-	(,256)	1024
ReLU	-	(,256)	0
$FC_2$ (Dense)	256	(,256)	65792
$BN_2$ (Batch normalization)	-	(,256)	1024
ReLU	-	(,256)	0
$FC_3$ (Dense)	32	(,32)	8224
$BN_3$ (Batch normalization)	-	(,32)	128
ReLU	-	(,32)	0
Dropout	-	(,32)	0
$FC_4$ (Dense)	1	(,1)	33

## 5 Results and Discussion

Once the best model was obtained, unknown data (i.e. data that were neither used in training nor in validation) were used to evaluate its performance. These correspond to the test dataset, i.e. 74850 samples, as explained above. With each of these samples, the respective prediction was performed using the trained

model, comparing its result with the real value, and the results were consolidated in a binary confusion matrix (see Table 4). In this matrix, TP (True Positives) corresponds to pixels that are correctly classified as moderate susceptibility, TN (True Negatives) corresponds to points that are correctly classified as high susceptibility, FP (False Positives) corresponds to pixels that are incorrectly classified as moderate susceptibility, while FN (False Negatives) corresponds to pixels that are incorrectly classified as high susceptibility. From the confusion matrix, the classifier evaluation metrics shown in Table 4 can be calculated using Eqs. 4–7 [18, 22].

**Table 4.** Confusion matrix and evaluation metrics for the test set.

		True condition	
		Moderate susceptibility	High susceptibility
Predicted condition	Moderate susceptibility	54861	15820
	High susceptibility	1541	2628
		Accuracy (ACC)	0.7681
		Precision (P)	0.7762
		Recall (R)	0.9727
		F1-Score (F <sub>1</sub> )	0.8634

Thus, accuracy corresponds to the percentage of correct classifications, precision to the percentage of classifications in the positive class (moderate susceptibility) that are true positives, and recall corresponds to the proportion of positives that are correctly identified [2]. In a classification task it is desirable that P and R reach the highest possible value, while being similar to each other. The ideal value in each case is 1 and the minimum value is 0. To evaluate the balance between them, the F1 score corresponding to the harmonic mean between P and R is calculated.

$$ACC = (TP + TN)/(TP + TN + FP + FN) \quad (4)$$

$$P = TP/(TP + FP) \quad (5)$$

$$R = TP/(TP + FN) \quad (6)$$

$$F_1 = 2(P \times R)/(P + R) \quad (7)$$

According to the evaluation results, the model is able to correctly classify most of the moderate susceptibility zones. In the case of high susceptibility zones, there are pixels that are classified as moderate susceptibility, which is mainly due to the absence of slope data (e.g. a digital elevation model), or geology and geomorphology data, which were key to build the ground truth data and are

not captured by a multispectral image. Beyond this, the zones detected by the model as high susceptibility largely reflect the areas classified in the elaboration of the ground truth data, as shown in the example in Fig. 4.

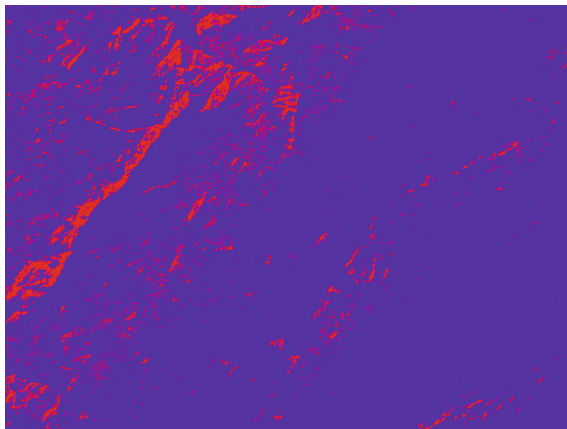


**Fig. 4.** Example of a landslide susceptibility map obtained using the proposed AutoML model for the study area. Red: high susceptibility, Violet: moderate susceptibility. (Color figure online)

Given the high variability of the susceptibility of ground truth data (Fig. 3b), the problem of identifying such zones becomes complex for a classifier fed only by multispectral data. This is reflected in the number of false negatives and positives. Hence, although the method can be used to obtain a general overview of the landslide susceptibility of an area, for greater accuracy the data must be complemented with other types of information.

## 6 Conclusion

The proposed model allows estimating susceptibility to mass movements, even without slope information or specific geological or geomorphological information. Since the response is obtained only from multispectral information, the susceptibility estimation is performed in a binary map (moderate or high susceptibility), while allowing to obtain such information only from one image. The model adjustment was performed using AutoML (AutoKeras) and achieved an F1 Score close to 86%.

**Acknowledgment.** This research was funded by “Vicerrectoría de Investigaciones–Universidad Militar Nueva Granada”, grant number INV-ING-3190 of 2020.

## References

1. Andreani, L., Stanek, K.P., Gloaguen, R., Krentz, O., Domínguez-González, L.: DEM-based analysis of interactions between tectonics and landscapes in the ore mountains and Eger Rift (East Germany and NW Czech Republic). *Remote Sens.* **6**(9), 7971–8001 (2014)
2. Ballesteros, D.M., Rodríguez-Ortega, Y., Renza, D., Arce, G.: Deep4SNet: deep learning for fake speech classification. *Expert Syst. Appl.* **184**, 115465 (2021). <https://doi.org/10.1016/j.eswa.2021.115465>
3. Beguería, S.: Changes in land cover and shallow landslide activity: a case study in the Spanish Pyrenees. *Geomorphology* **74**(1–4), 196–206 (2006)
4. Chollet, F., et al.: Keras. <https://keras.io> (2015)
5. Chung, C.J.F., Fabbri, A.G., et al.: Probabilistic prediction models for landslide hazard mapping. *Photogram. Eng. Remote Sens.* **65**(12), 1389–1399 (1999)
6. Corominas, J., et al.: Recommendations for the quantitative analysis of landslide risk. *Bull. Eng. Geol. Environ.* **73**(2), 209–263 (2014)
7. Cuervo, G.V.: Evaluación de imágenes de satélite sar ers-1 y spot-landsat en la cartografía de movimientos en masa. In: *The Use and Applications of ERS in Latin America*, p. 109. ESTEC Publishing Division (1997)
8. Esper Angillieri, M.Y.: Inventario de procesos de remoción en masa de un sector del departamento iglesia, san juan. *Revista de la Asociación Geológica Argentina* **68**(2), 225–232 (2011)
9. Guzzetti, F., Mondini, A.C., Cardinali, M., Fiorucci, F., Santangelo, M., Chang, K.T.: Landslide inventory maps: new tools for an old problem. *Earth-Sci. Rev.* **112**(1–2), 42–66 (2012)
10. Jin, H.: Efficient neural architecture search for automated deep learning. Ph.D. thesis, Texas A&M University (2021)
11. Jin, H., Song, Q., Hu, X.: Auto-Keras: an efficient neural architecture search system. In: *Proceedings of the 25th ACM SIGKDD International Conference on Knowledge Discovery & Data Mining*, pp. 1946–1956. ACM (2019)
12. Keyport, R.N., Oommen, T., Martha, T.R., Sajinkumar, K., Gierke, J.S.: A comparative analysis of pixel-and object-based detection of landslides from very high-resolution images. *Int. J. Appl. Earth Observ. Geoinf.* **64**, 1–11 (2018)
13. Nichol, J., Wong, M.S.: Satellite remote sensing for detailed landslide inventories using change detection and image fusion. *Int. J. Remote Sens.* **26**(9), 1913–1926 (2005)
14. Ospina-Gutiérrez, J.P., Aristizábal, E.: Aplicación de inteligencia artificial y técnicas de aprendizaje automático para la evaluación de la susceptibilidad por movimientos en masa. *Revista Mexicana De Ciencias Geológicas* **38**(1), 43–54 (2021)
15. Paolini, L., Sobrino, J.A., Jimenez Muños, J.C.: Detección de deslizamientos de ladera mediante imágenes landsat tm: El impacto de estos disturbios sobre los bosques subtropicales del noroeste de argentina. *Revista de Teledetección* (2002)
16. de Planeación, D.N.: Índice municipal de riesgo de desastres ajustado por capacidades (2019). <https://colaboracion.dnp.gov.co/CDT/Prensa/IndicemunicipalRiesgos.pdf>
17. Recondo, C., Menéndez, C., García, P., González, R., Sáez, E.: Estudio de las zonas propensas a sufrir deslizamientos en los concejos de oviedo y mieres (asturias) a partir de una imagen landsat-tm y de un modelo digital de elevaciones. *Rev Teledetec* **14**, 49–59 (2000)

18. Rodriguez-Ortega, Y., Ballesteros, D.M., Renza, D.: Copy-move forgery detection (CMFD) using deep learning for image and video forensics. *J. Imaging* **7**(3), 59 (2021)
19. Sameen, M.I., Pradhan, B.: Landslide detection using residual networks and the fusion of spectral and topographic information. *IEEE Access* **7**, 114363–114373 (2019)
20. Servicio-Geológico-Colombiano: Documento metodológico de la zonificación de susceptibilidad y amenaza por movimientos en masa, escala 1:100.000 (2013). <https://www.sgc.gov.co>
21. Servicio-Geológico-Colombiano: Lineamientos técnicos para elaboración de mapas de amenaza por movimientos en masa a escala municipal y rural (2013). <https://www.sgc.gov.co>
22. Ulloa, C., Ballesteros, D.M., Renza, D.: Video forensics: identifying colorized images using deep learning. *Appl. Sci.* **11**(2), 476 (2021)
23. Wang, H., Zhang, L., Luo, H., He, J., Cheung, R.: AI-powered landslide susceptibility assessment in Hong Kong. *Eng. Geol.* **288**, 106103 (2021)